ANNALES DE L'INSTITUT FOURIER

Hans U. Boden & Homayun Karimi

The Jones–Krushkal polynomial and minimal diagrams of surface links

THE JONES–KRUSHKAL POLYNOMIAL AND MINIMAL DIAGRAMS OF SURFACE LINKS

by Hans U. BODEN & Homayun KARIMI (*)

––––––––

ABSTRACT. — We prove a Kauffman–Murasugi-Thistlethwaite theorem for alternating links in thickened surfaces. It implies that any reduced alternating diagram of a link in a thickened surface has minimal crossing number, and any two reduced alternating diagrams of the same link have the same writhe. This result is proved more generally for link diagrams that are adequate, and the proof involves a two-variable generalization of the Jones polynomial for surface links defined by Krushkal. The main result is used to establish the first and second Tait conjectures for links in thickened surfaces and for virtual links.

RÉSUMÉ. — Nous montrons un théorème de Kauffman-Murasugi-Thistlethwaite pour des entrelacs alternants dans des voisinages tubulaires d'une surface. Il implique que tout diagramme réduit d'entrelacs alternant dans une surface a un nombre minimal de croisements, et que deux diagrammes réduits alternants quelconques du même entrelacs ont le même nombre d'auto-enlacements.

Ce résultat est prouvé plus généralement pour les diagrammes d'entrelacs qui sont adéquats, et sa démonstration utilise une généralisation à deux variables du polynôme de Jones pour les entrelacs sur des surfaces définies par Krushkal. Le résultat principal est utilisé pour établir la première et la deuxième conjecture de Tait pour les entrelacs dans des voisinages tubulaires d'une surface et pour les entrelacs virtuels.

Introduction

A link diagram is called *alternating* if the crossings alternate between over and under crossing as one travels around any component; any link admitting such a diagram is called *alternating*. In his early work of tabulating knots [33], Tait formulated several far-reaching conjectures which, when resolved 100 years later, effectively solved the classification problem

for alternating knots and links. Recall that a link diagram is said to be *reduced* if it does not contain any nugatory crossings. Tait's first conjecture states that any reduced alternating diagram of a link has minimal crossing number. His second states that any two such diagrams representing the same link have the same writhe. His third conjecture, also known as the Tait flyping conjecture, asserts that any two reduced alternating diagrams for the same link are related by a sequence of flype moves (see Figure 5.1).

Tait's first and second conjectures were settled through results of Kauffman, Murasugi, and Thistlethwaite, who each gave an independent proof using the newly discovered Jones polynomial [19, 30, 34]. The Tait flyping conjecture was subsequently solved by Menasco and Thistlethwaite [29], and taken together, the three Tait conjectures provide an algorithm for classifying alternating knots and links. A striking corollary is that the crossing number is additive under connected sum for alternating links. It remains a difficult open problem to prove this in general for arbitrary links in S^3.

Virtual knots were introduced by Kauffman in [20], and they represent a natural generalization of classical knot theory to knots in thickened surfaces up to stabilization. Classical knots and links embed faithfully into virtual knot theory [11], and many invariants from classical knot theory extend in a natural way. For instance, the Jones polynomial was extended to virtual links by Kauffman [20], who noted the abundant supply of virtual knots with trivial Jones polynomial. (For classical knots, it is an open problem whether there is a nontrivial knot with trivial Jones polynomial.) Indeed, there exist alternating virtual knots K with trivial Jones polynomial (and even trivial Khovanov homology [18]). Consequently, the Jones polynomial is not sufficiently strong to prove the analogue of the Kauffman–Murasugi–Thistlethwaite theorem for virtual links (see also [15] and [9]).

The main result in this paper is an analogue of the Kauffman–Murasugi–Thistlethwaite theorem for reduced alternating links in thickened surfaces. It is established using a two-variable generalization of the Jones polynomial for links in thickened surfaces defined by Krushkal [22]. The Jones–Krushkal polynomial is a homological refinement of the usual Jones polynomial in that it records the homological ranks of the states under restriction to the background surface. It is derived from Krushkal's extension of the Tutte polynomial to graphs in surfaces [22]. The main result can be paraphrased in terms of homological Kauffman bracket $\langle \cdot \rangle_\Sigma$ as follows (see Theorem 4.1 and Corollary 4.6):

Theorem. — *If L is an oriented link in a thickened surface $\Sigma \times I$ of genus g, and if D is a connected link diagram for L with n crossings, then*

$$\operatorname{span}(\langle D \rangle_\Sigma) \leqslant 4n - 4 + 4g,$$

with equality if D is reduced and alternating.

In particular, any reduced alternating diagram for L has minimal crossing number, and any two reduced alternating diagrams for L have the same writhe.

The main result is proved more generally for diagrams that are adequate in a certain sense (see Definition 2.5), and we show that every reduced alternating diagram of a link in a thickened surface is adequate (Proposition 2.8). In the last section, Corollary 4.6 is applied to prove the Tait conjectures for virtual knots and links (see Theorem 5.2 and 5.3).

In [3], Adams et al. use geometric methods to prove minimality of reduced alternating diagrams of knots in thickened surfaces. In this paper, we recover and extend the results in [3] to links in thickened surfaces admitting adequate diagrams. A key step is provided by the dual state lemma for links in thickened surfaces (Lemma 2.10), and its proof relies on an analysis of the homological Kauffman bracket and Jones–Krushkal polynomial. These invariants are closely related to the surface bracket polynomial studied in [10] and [25]. However, they exhibit different behavior in that they are not invariant under stabilization and destabilization. In [22], Krushkal shows that the Jones–Krushkal polynomial admits an interpretation in terms of the generalized Tutte polynomial of the associated Tait graph. This result is a generalization of Thistlethwaite's theorem [34]. In a similar vein, Chmutov and Voltz show how to relate the Jones polynomial of a checkerboard colorable virtual link with the Bollabás–Riordan polynomial of its Tait graph in [8] (see also [7]).

We close this introduction with a brief synopsis of the contents of the rest of this paper. In Section 1, we review background material on links in thickened surfaces and virtual links. One result characterizes checkerboard colorable virtual links (Proposition 1.7) In Section 2, we recall the definition of the homological Kauffman bracket $\langle \cdot \rangle_\Sigma$ and show that it is invariant under regular isotopy. We prove that every reduced alternating link diagram is adequate (Proposition 2.8) and establish the dual state lemma (Lemma 2.10). In Section 3, we introduce the Jones–Krushkal polynomial $\widetilde{J}(t, z) \in \mathbb{Z}[t^{1/2}, t^{-1/2}, z]$ and show that it is an invariant of links in thickened surfaces up to isotopy and diffeomorphism. For checkerboard colorable links, we introduce the *reduced* Jones–Krushkal polynomial $J(t, z)$

and give many sample calculations of $\widetilde{J}(t,z)$ and $J(t,z)$. We prove that the Jones–Krushkal polynomial of L is closely related to that of its mirror images L^* and $L^\dagger$ (Proposition 3.12).

Section 4 contains the proof of the main result, which is the Kauffman–Murasugi–Thistlethwaite theorem for reduced alternating link diagrams on surfaces (Theorem 4.1 and Corollary 4.6). In Section 5, we apply the main result to deduce the first and second Tait conjectures for virtual links (Theorem 5.3). Tables 5.1 and 5.2 list the unreduced and reduced Jones–Krushkal polynomials for all virtual knots with 3 crossings and all checkerboard colorable virtual knots with 4 crossings.

Notation. — Unless otherwise specified, all homology groups are taken with $\mathbb{Z}/2$ coefficients. Decimal numbers such as 3.5 and 4.98 refer to the virtual knots in Green's tabulation [12].

1. Virtual links and links in thickened surfaces

In this section, we review the basic properties of virtual links and links in thickened surfaces.

1.1. Virtual link diagrams

A virtual link diagram is an immersion of $m \geqslant 1$ circles in the plane with only double points, such that each double point is either classical (indicated by over- and under-crossings) or virtual (indicated by a circle around the double point). Two virtual link diagrams are said to be equivalent if they can be related by planar isotopies, Reidemeister moves, and the *detour move* shown in Figure 1.1. (See [20] for more details.) An oriented virtual link L includes a choice of orientation for each component of L, which is indicated by placing arrows on the components as in Figure 1.2.

Given a virtual link diagram D, the crossing number is denoted $c(D)$ and is defined to be the number of classical crossings of D. The *crossing number* of a virtual link L is the minimum crossing number $c(D)$ taken over all virtual link diagrams D representing L.

Given an oriented virtual link, each classical crossing is either positive or negative, see Figure 1.3. The writhe of the crossing is ± 1 according to whether the crossing is positive or negative. The writhe of the diagram is the sum of the writhes of all its crossings.
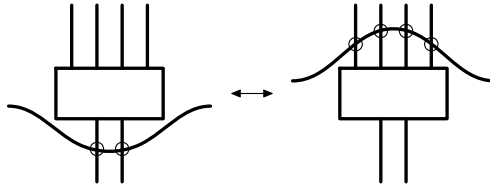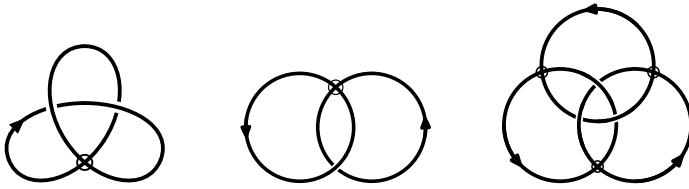
Figure 1.1. The detour move.

Figure 1.2. The virtual trefoil, Hopf link, and Borromean rings.

DEFINITION 1.1. — *For a virtual link diagram D, the* writhe *of D, denoted $w(D)$ is defined as $n_+(D) - n_-(D)$, where $n_+(D)$ and $n_-(D)$ are the number of positive and negative crossings in D, respectively.*

Figure 1.3. A positive and a negative crossing.

1.2. Links in thickened surfaces

Virtual links can also be defined as equivalence classes of links in thickened surfaces. Let $I = [0, 1]$ denote the unit interval and Σ be a compact, connected, oriented surface. A *link in the thickened surface* $\Sigma \times I$ is an embedding $L \colon \bigsqcup_{i=1}^{m} S^1 \hookrightarrow \Sigma \times I$, considered up to isotopy and orientation preserving homeomorphisms of the pair $(\Sigma \times I, \Sigma \times \{0\})$.

A *surface link diagram* on Σ is a tetravalent graph in Σ whose vertices indicate over and under crossings in the usual way. Two surface link diagrams represent isotopic links if and only if they are equivalent by local

Reidemeister moves. The writhe of a link diagram on a surface is defined in the same way as it is for virtual links (cf. Definition 1.1).

Framed links in $\Sigma \times I$ are represented by link diagrams on Σ up to *regular isotopy*. Recall that two link diagrams on Σ are regularly isotopic if they are related by a sequence of moves that involve Reidemeister 2 and 3 moves and the writhe-preserving move in Figure 1.4. Notice that the writhe is invariant under regular isotopy of links in $\Sigma \times I$.

Figure 1.4. Regular isotopy includes the above move together with Reidemeister 2 and 3 moves.

Let $p \colon \Sigma \times I \to \Sigma$ be projection onto the first factor. The image $p(L) \subset \Sigma$ is called the *projection* of the link. Using an isotopy, we can arrange that the projection is a regular immersion with finitely many double points.

Two links $L_0 \subset \Sigma_0 \times I$ and $L_1 \subset \Sigma_1 \times I$ are said to be *stably equivalent* if one is obtained from the other by a finite sequence of isotopies, diffeomorphisms, stabilizations, and destabilizations. Stabilization is the operation of adding a 1-handle to Σ to obtain a new surface Σ', and destabilization is the opposite procedure. Specifically, if D_0 and D_1 are two disjoint disks in Σ which are both disjoint from the image of L under projection $\Sigma \times I \to \Sigma$, then Σ' is the surface with $\mathrm{genus}(\Sigma') = \mathrm{genus}(\Sigma) + 1$ obtained by attaching an annulus $A = S^1 \times I$ to $\Sigma \smallsetminus (D_0 \cup D_1)$ so that $\partial A = \partial D_0 \cup \partial D_1$. This operation is referred to as *stabilization*, and the opposite procedure is called *destabilization*. It involves cutting along a vertical annulus in $\Sigma \times I$ disjoint from the link and attaching two 2-disks.

In [6], Carter, Kamada, and Saito give a one-to-one correspondence between virtual links and stable equivalence classes of links in thickened surfaces. The next result is Kuperberg's theorem [23].

THEOREM 1.2. — *Every stable equivalence class of links in thickened surfaces has a unique irreducible representative.*

Given a virtual link L, its virtual genus $g_v(L)$ is defined to be the genus of the surface of its unique irreducible representative. A virtual link L is said to be *classical* if it has virtual genus $g_v(L) = 0$. This is the case if and only if it can be represented by a virtual link diagram with no virtual crossings. For instance, the three virtual links in Figure 1.2 all have virtual genus equal to one and so are non-classical (see Figures 3.2, 2.2, and 3.3).

There is a construction, due to Kamada and Kamada [16], which associates to any virtual link diagram D a ribbon graph on an oriented surface. The graph is a tetravalent graph representing the projection of D, and the surface M_D has a handlebody decomposition with 0-handles being disk neighborhoods of each of the real crossings of D, and 1-handles for each of the arcs of D from one crossing to the next. If D has n crossings, then M_D has n 0-handles and $2n$ 1-handles. Let Σ_D denote the closed oriented surface obtained by attaching disks to all the boundary components of M_D. A diagram D for a virtual link L is said to be a *minimal genus diagram* if the genus of Σ_D is equal to the virtual genus of L.

Notice that under this construction, the link diagram is cellularly embedded in Σ_D, namely the complement of its projection is a union of disks. By Theorem 1.2, this will be true for any minimal genus diagram of a virtual link L.

1.3. Alternating virtual links

A virtual link diagram D is said to be *alternating* if, when traveling along the components, the classical crossings alternate from over to under when one disregards the virtual crossings. A virtual link L is *alternating* if it can be represented by an alternating virtual link diagram.

In a similar way, a surface link diagram D on Σ is said to be *alternating* if the crossings alternate from over to under around any component of D. It follows that a virtual link is alternating if and only if it can be represented by an alternating surface link diagram.

DEFINITION 1.3. — *Let D be a surface link diagram on Σ. A crossing c in D is called* nugatory *if we can find a simple closed curve in Σ which separates Σ and intersects D only in the double point c.*

Remark 1.4. — For classical link diagrams, nugatory crossings can always be removed by rotating one side of the diagram 180° relative to the other. In contrast, for link diagrams on surfaces, nugatory crossings are not in general removable.

DEFINITION 1.5. — *A surface link diagram D on Σ is called* reduced *if it is cellularly embedded and has no nugatory crossings.*

Remark 1.6. — Note that, by the Kamada–Kamada construction, any virtual link can be realized by a cellularly embedded diagram on a surface. Thus, the first condition of Definition 1.5 can always be arranged for virtual links.
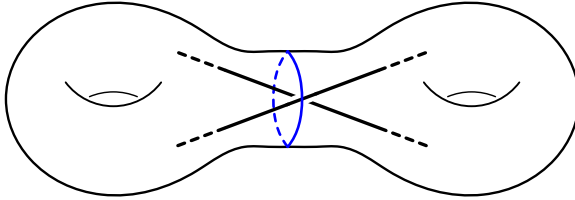
Figure 1.5. A nugatory crossing.

1.4. Checkerboard colorable links

A surface link diagram D on Σ is said to be *checkerboard colorable* if the components of $\Sigma \smallsetminus D$ can be colored by two colors such that any two components of $\Sigma \smallsetminus D$ that share an edge have opposite colors. A link in a thickened surface is checkerboard colorable if it can be represented by a checkerboard colorable surface link diagram. Likewise, a virtual link is checkerboard colorable if it admits a checkerboard colorable representative.

In [14], Kamada showed that every alternating virtual link is checkerboard colorable. In fact, in [14, Lemma 7] she showed that a virtual link diagram is checkerboard colorable if and only if it can be transformed into an alternating diagram under crossing changes.

There are, however, subtle differences between the categories of virtual links and links in thickened surfaces. For instance, Kamada's results hold for links in thickened surfaces provided they are cellularly embedded, but as we shall see, they can fail without this assumption. For instance, Figure 1.6 presents an alternating knot diagram on the torus which is not checkerboard colorable, hence Kamada's result is *not* true in general. The failure stems from the fact that this diagram is not cellularly embedded. In particular, the diagram in Figure 1.6 is not minimal genus, and any vertical arc disjoint from the knot gives a destabilizing curve. Destabilization along this curve shows that this knot is stably equivalent to the classical trefoil, which of course is checkerboard colorable.

Several authors have used slightly different names for the notion of checkerboard colorability. For instance, in [17], checkerboard colorable links are called *normal*, and in [31], checkerboard colorable diagrams are called *even*. In [4], checkerboard colorable links are called mod 2 almost classical links.

Suppose that D is a surface link diagram on Σ which is cellularly embedded and checkerboard colorable, and fix a checkerboard coloring of the complementary regions of D in Σ. The black regions determine a spanning
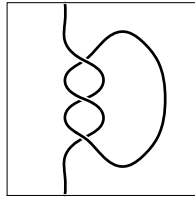
Figure 1.6. An alternating knot diagram on the torus which is not checkerboard colorable.

surface for L which is the union of disks and bands, with one disk for each black region and one half-twisted band for each crossing.

The result is an unoriented surface F embedded in $\Sigma \times I$ with boundary $\partial F = L$. Associated to this surface is its Tait graph Γ, which is a graph embedded in Σ with one vertex for each black region and one edge for each crossing. There is an edge between two vertices for each crossing connecting the corresponding regions. In particular, if a black region has a self-abutting crossing, then its Tait graph Γ will contain a loop.

The dual spanning surface for L can be constructed by starting with the white regions and adding half-twisted bands for each crossing. Its Tait graph is defined similarly. The black and white Tait graphs are dual graphs in the surface Σ, and each of the checkerboard surfaces deformation retracts onto its Tait graph. The next result gives a useful characterization of checkerboard colorability for links in thickened surfaces.

PROPOSITION 1.7. — *Given a link $L \subset \Sigma \times I$ in a thickened surface, the following are equivalent:*

   (i) *L is checkerboard colorable.*
   (ii) *L is the boundary of an unoriented spanning surface $F \subset \Sigma \times I$.*
   (iii) *$[L] = 0$ in the homology group $H_1(\Sigma \times I; \mathbb{Z}/2)$.*

Proof. — If L is checkerboard colorable, then an unoriented spanning surface is obtained by attaching one half-twisted band between two black regions for each crossing of L. This shows that (i) $\Rightarrow$ (ii), and to see the reverse implication, suppose that F is a spanning surface for L, realized as a union of disks and bands in $\Sigma \times I$. Perform an isotopy to shrink the disks and bands so the images of the disks under projection $p \colon \Sigma \times I \to \Sigma$ are disjoint from one another and from each band. Thus, the projection, restricted to F, is an embedding except for band crossings. At each band crossing, we can attach a 1-handle as in Figure 1.7 so that the new surface

is the black surface for a checkerboard coloring of the resulting diagram of L. Thus (ii) $\Rightarrow$ (i).

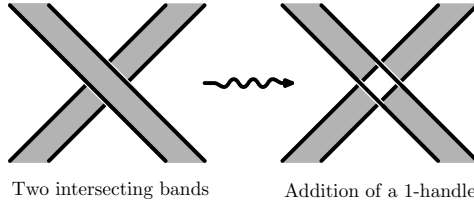<div align="center">Two intersecting bands   Addition of a 1-handle</div>

Figure 1.7. Adding a vertical 1-handle at a band crossing.

The step (ii) $\Rightarrow$ (iii) is obvious, and the reverse implication follows from a standard argument which is left to the reader. $\qquad\square$

2. The homological Kauffman bracket

In this section, we recall the definition of the homological Kauffman bracket from [22]. It is defined for link diagrams in thickened surfaces and is an invariant of *regular isotopy* of unoriented links. We introduce a notion of adequacy for link diagrams on surfaces and use the homological bracket to prove that adequate link diagrams have minimal crossing number.

2.1. States and their homological rank

Let L be a link in $\Sigma \times I$ with surface link diagram D on Σ. Suppose further that D has n crossings. For each crossing c_i of D, there are two ways to resolve it. One is called the *A-smoothing* and the other is the *B-smoothing*, according to Figure 2.1.

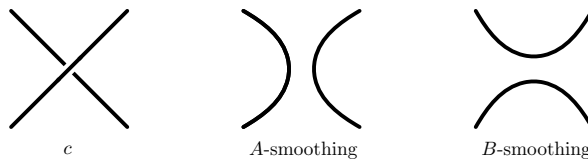<div align="center">c *A*-smoothing   *B*-smoothing</div>

Figure 2.1. The A- and B-smoothing of a crossing.

A *state* is a collection of simple closed curves on Σ which results from smoothing each of the crossings of D. Thus, a state S is just a link diagram

on Σ with no crossings. Since there are two ways to smooth each crossing, there are 2^n states. We will use $\mathfrak{S} = \mathfrak{S}(D)$ to denote the space of all states of D. Ordering the crossings $\{c_1, \ldots, c_n\}$ of D in an arbitrary way, we can identify each state with a binary word $\varepsilon_1 \varepsilon_2 \cdots \varepsilon_n$ of length n, where $\varepsilon_i = 0$ indicates an A-smoothing and $\varepsilon_i = 1$ a B-smoothing at the crossing c_i.

Given a state $S \in \mathfrak{S}$, let $a(S)$ be the number of A-smoothings and $b(S)$ the number of B-smoothings, and let $|S|$ be the number of cycles in S. Define

$$k(S) = \dim\left(\operatorname{kernel}\left(i_* \colon H_1(S) \longrightarrow H_1(\Sigma)\right)\right),$$
$$r(S) = \dim\left(\operatorname{image}\left(i_* \colon H_1(S) \longrightarrow H_1(\Sigma)\right)\right),$$

where $i \colon S \to \Sigma$ is the inclusion map. We call $r(S)$ the *homological rank* of the state S, and we note that $k(S) + r(S) = b_1(S) = |S|$.

Since Σ is a compact, closed, oriented surface, the intersection pairing on $H_1(\Sigma)$ is symplectic. A given collection of disjoint simple closed curves on Σ must therefore map into an isotropic subspace of $H_1(\Sigma)$. It follows that the homological rank of any state S satisfies $0 \leqslant r(S) \leqslant g$, where g is the genus of Σ.

The *homological Kauffman bracket* is denoted $\langle \cdot \rangle_\Sigma$ and defined by setting

$$(2.1) \qquad \langle D \rangle_\Sigma = \sum_{S \in \mathfrak{S}} A^{(a(S) - b(S))} (-A^{-2} - A^2)^{k(S)} z^{r(S)}.$$

Here, z is a formal variable which keeps track of the homological rank of S. Upon setting $z = -A^{-2} - A^2$ and dividing one factor of $-A^{-2} - A^2$, one recovers the usual Kauffman bracket.

The following lemmas study the effect of the various diagrammatic moves on the homological Kauffman bracket. These will be applied to show that it is invariant under regular isotopy of links in surfaces. The first is an immediate consequence of Equation (2.1), and the proof is left to the reader.

In the first lemma, $\bigcirc$ denotes a simple closed curve on Σ.

LEMMA 2.1. — *The homological Kauffman bracket satisfies the following identities.*

(i) *If $\bigcirc$ is homologically trivial, then $\langle \bigcirc \rangle_\Sigma = -A^2 - A^{-2}$. Otherwise,*
$\langle \bigcirc \rangle_\Sigma = z$.

(ii) *If $\bigcirc$ is homologically trivial, then $\langle \bigcirc \sqcup L \rangle_\Sigma = (-A^2 - A^{-2}) \langle L \rangle_\Sigma$.*

(iii) $\left\langle \times \right\rangle_\Sigma = A \left\langle \,\right)\left(\,\right\rangle_\Sigma + A^{-1} \left\langle \asymp \right\rangle_\Sigma.$

LEMMA 2.2. — *If a link diagram on a surface is changed by a Reidemeister type 1 move, then the homological Kauffman bracket changes as follows:*

$$(2.2) \quad \left\langle \vcenter{\hbox{\includegraphics{curl1}}} \right\rangle_\Sigma = -A^3 \left\langle \vcenter{\hbox{\includegraphics{arc}}} \right\rangle_\Sigma \quad and \quad \left\langle \vcenter{\hbox{\includegraphics{curl2}}} \right\rangle_\Sigma = -A^{-3} \left\langle \vcenter{\hbox{\includegraphics{arc}}} \right\rangle_\Sigma.$$

Proof. — To see the first identity, apply Lemma 2.1 (iii) to the left-hand side of Equation (2.2) and simplify using Lemma 2.1 (ii). The first equation follows immediately. The second identity follows by a similar argument; details are left to the reader. ☐

LEMMA 2.3. — *If a link diagram on a surface is changed by a Reidemeister type 2 or 3 move, then the homological Kauffman bracket is unchanged, i.e., we have*

(i) $\left\langle \vcenter{\hbox{\includegraphics{r2l}}} \right\rangle_\Sigma = \left\langle \vcenter{\hbox{\includegraphics{r2r}}} \right\rangle_\Sigma$, *and*

(ii) $\left\langle \vcenter{\hbox{\includegraphics{r3l}}} \right\rangle_\Sigma = \left\langle \vcenter{\hbox{\includegraphics{r3r}}} \right\rangle_\Sigma$

Proof. — To prove (i), apply Lemma 2.1 (iii) twice to the diagram on the left and simplify using Lemma 2.1 (ii). The identity (i) follows.

To prove (ii), apply Lemma 2.1 (iii) to the lower crossing in the diagram on the left and simplify, using the fact that $\langle \cdot \rangle_\Sigma$ is invariant under Reidemeister 2 moves. The identity (ii) then follows. ☐

Lemma 2.3 implies that the bracket $\langle D \rangle_\Sigma$ is an invariant of unoriented links in $\Sigma \times I$ up to *regular* isotopy, and in Definition 3.1 we use Lemma 2.2 to define a normalization which is an invariant of oriented links in $\Sigma \times I$ up to isotopy.
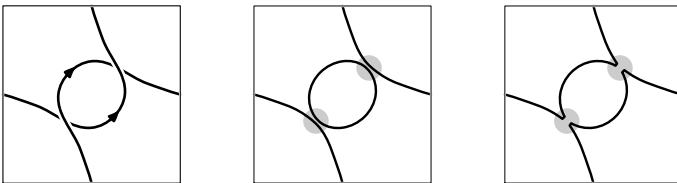

Figure 2.2. *A minimal genus diagram of the virtual trefoil in the torus, and the states S_A and S_B.*

Example 2.4. — The virtual trefoil K (see Figure 1.2) admits a minimal genus diagram D on the torus T, which has two crossings. The diagram D is depicted in Figure 2.2, along with the state S_A of pure A smoothings and

the state S_B of pure B-smoothings. Clearly $|S_A| = 2, r(S_A) = 1$ and $|S_B| = 1, r(S_B) = 1$. One can further show that the other two states AB, BA have $|S| = 1$ and $r(S) = 1$. Thus, $\langle D \rangle_T = A^2(-A^2 - A^{-2})z + 2z + A^{-2}z$.

Notice that the cube of resolutions for this knot has single cycle smoothings. These occur whenever there are two states S, S' with $|S| = |S'|$ which are identical everywhere except one crossing. For checkerboard colorable diagrams, one can show that $|S| = |S'| \pm 1$ whenever S, S' are two states that differ only at one crossing (for a proof, see [18, Proposition 5.11]). Therefore, the cube of resolutions of a checkerboard colorable diagram never has any single cycle smoothings.

2.2. Adequate diagrams

Next, we introduce the notions of A-adequate and B-adequate for link diagrams on a surface. In the following, for a given link diagram D on a surface, let S_A denote the pure A-smoothing state and S_B the pure B-smoothing state.

We take a moment to review the state-sum formulation for the homological Kauffman bracket. Given a link diagram D on Σ and a state $S \in \mathfrak{S}(D)$, let

$$(2.3) \qquad \langle D \,|\, S \rangle_\Sigma = A^{(a(S)-b(S))}(-A^{-2} - A^2)^{k(S)}z^{r(S)}.$$

Then we can write

$$(2.4) \qquad \langle D \rangle_\Sigma = \sum_{S \in \mathfrak{S}} \langle D \,|\, S \rangle_\Sigma.$$

DEFINITION 2.5. — *The diagram D is called A-adequate, if for any state S' with exactly one B-smoothing, we have $k(S') \leqslant k(S_A)$. The diagram D is called B-adequate if, for any state S' with exactly one A-smoothing, we have $k(S') \leqslant k(S_B)$. A diagram is called adequate if it is both A- and B-adequate.*

Recall that for a classical link, a link diagram D is "plus-adequate" if the pure A-smoothing state S_A does not contain any self-abutting cycles, and it is "minus-adequate" if the same holds for the pure B-smoothing state S_B [24, Definition 5.2]. Thus, if a diagram is plus-adequate then it is A-adequate, and if it is minus-adequate then it is B-adequate.

However, a diagram can be A-adequate without being plus-adequate, and it can be B-adequate without being minus-adequate. Indeed, our notion of adequacy is less restrictive because it allows self-abutting cycles in S_A

provided that $k(S') \leqslant k(S_A)$ for the new state S' obtained by switching the smoothing. In case $|S'| = |S_A| + 1$, this is equivalent to the requirement that $r(S') = r(S_A) + 1$. There is a similar interpretation for B-adequacy.

In [15, p. 1089], Kamada defines a virtual link diagram to be *proper* if four distinct regions of the complement meet at every crossing. Any virtual link diagram that is proper is automatically adequate according to Definition 2.5, but the converse is not true in general. Indeed, in Proposition 2.8, we will show that all reduced alternating link diagrams on surfaces are adequate, whereas most alternating knot diagrams on surfaces are not proper.

We use $d_{\max}$ and $d_{\min}$ to denote the maximal and minimal degree in the variable A. For example, $d_{\max}(\langle D \,|\, S \rangle_\Sigma) = a(S) - b(S) + 2k(S)$ and $d_{\min}(\langle D \,|\, S \rangle_\Sigma) = a(S) - b(S) - 2k(S)$. (Note that the homological variable z is disregarded in degree considerations.)

LEMMA 2.6. — *If D is a surface link diagram on Σ with n crossings, then*

(i) $d_{\max}(\langle D \rangle_\Sigma) \leqslant n + 2k(S_A)$, *with equality if D is A-adequate,*
(ii) $d_{\min}(\langle D \rangle_\Sigma) \geqslant -n - 2k(S_B)$, *with equality if D is B-adequate.*

Proof. — Suppose that S is a state for D with an A-smoothing at a given crossing but otherwise arbitrary, and let S' be the state obtained by switching it to a B-smoothing at the given crossing. Clearly, $a(S') = a(S) - 1$ and $b(S') = b(S) + 1$. Switching the crossing produces a cobordism from S to S', and there are three possibilities:

(a) two cycles in S join to form one cycle in S',
(b) one cycle in S splits to form two cycles in S', or
(c) switching from S to S' involves a single cycle smoothing (see Figure 2.3).

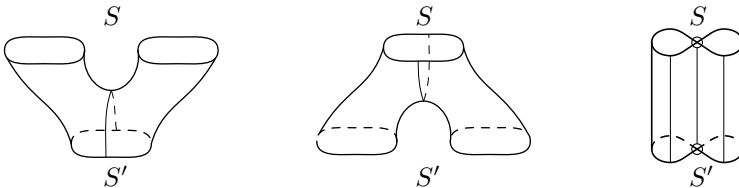Notice that $|S'| = |S| - 1$, $|S'| = |S| + 1$, or $|S'| = |S|$ in cases (a), (b), or (c), respectively.

Figure 2.3. *The three types of cobordisms from S to S' include a fusion (left), fission (middle), and single cycle smoothing (right).*

Further, in case (a), either $r(S') = r(S)$ and $k(S') = k(S) - 1$ or $r(S') = r(S) - 1$ and $k(S') = k(S)$; and in case (b), either $r(S') = r(S)$ and $k(S') = k(S) + 1$ or $r(S') = r(S) + 1$ and $k(S') = k(S)$. In case (c), one can verify that $r(S') = r(S)$ and $k(S') = k(S)$. Since $a(S') - b(S') = a(S) - b(S) - 2$ and $k(S') \leqslant k(S) + 1$ in all three cases, we conclude that

$$(2.5) \qquad d_{\max}\left(\langle D \,|\, S' \rangle_\Sigma\right) \leqslant d_{\max}\left(\langle D \,|\, S \rangle_\Sigma\right).$$

Clearly $d_{\max}(\langle D \,|\, S_A \rangle_\Sigma) = n + 2k(S_A)$ and $d_{\min}(\langle D \,|\, S_B \rangle_\Sigma) = -n - 2k(S_B)$. Since any state is obtained from S_A by switching smoothings at a finite set of crossings, repeated application of Equation (2.5) gives that $d_{\max}(\langle D \,|\, S \rangle_\Sigma) \leqslant d_{\max}(\langle D \,|\, S_A \rangle_\Sigma)$, and the inequality (i) follows.

Now suppose that D is A-adequate and S is a state with exactly one B-smoothing. Then A-adequacy implies that $k(S) \leqslant k(S_A)$. Since $a(S) - b(S) = n - 2$, it follows that

$$(2.6) \qquad d_{\max}(\langle D \,|\, S \rangle_\Sigma) \leqslant d_{\max}(\langle D \,|\, S_A \rangle_\Sigma) - 2.$$

Any state S' with two or more B-smoothings is obtained from a state S with exactly one B-smoothing by switching the smoothings at the remaining crossings. Therefore, by Equations (2.5) and (2.6), we find that

$$d_{\max}(\langle D \,|\, S' \rangle_\Sigma) \leqslant d_{\max}(\langle D \,|\, S \rangle_\Sigma) \leqslant d_{\max}(\langle D \,|\, S_A \rangle_\Sigma) - 2.$$

Thus $d_{\max}(\langle D \rangle_\Sigma) = n + 2k(S_A)$, and this completes the proof of (i).

Statement (ii) follows by a similar argument. Alternatively, one can deduce (ii) directly from (i) using the observation that a diagram is A-adequate if and only if its mirror image is B-adequate. $\qquad\square$

Define the span of the homological Kauffman bracket by setting

$$\mathrm{span}(\langle D \rangle_\Sigma) = d_{\max}(\langle D \rangle_\Sigma) - d_{\min}(\langle D \rangle_\Sigma).$$

By Lemma 2.3, the homological Kauffman bracket is invariant under the second and third Reidemeister moves. Lemma 2.2 implies that $\mathrm{span}(\langle D \rangle_\Sigma)$ is also invariant under the first Reidemeister move. Therefore, it gives an invariant of the underlying link.

COROLLARY 2.7. — *If D is a link diagram with n crossings on a surface Σ, then*

$$\mathrm{span}(\langle D \rangle_\Sigma) \leqslant 2n + 2k(S_A) + 2k(S_B),$$

with equality if D is adequate.

PROPOSITION 2.8. — *Any reduced alternating diagram D for a link in a thickened surface $\Sigma \times I$ is adequate.*

Proof. — Any reduced alternating link diagram on a surface is checkerboard colorable, and one can choose the coloring so that the white regions are enclosed by the cycles of S_A and the black regions by the cycles of S_B. Since each cycle in S_A bounds a white region, it follows that S_A is homologically trivial. Thus $r(S_A) = 0$ and $k(S_A) = b_1(S_A) = |S_A|$. Similarly, since each cycle in S_B bounds a black region, S_B is also homologically trivial. Thus $r(S_B) = 0$ and $k(S_B) = b_1(S_B) = |S_B|$.

We will now show that D is A-adequate. Suppose that S is a state with exactly one B-smoothing. Then $|S| = |S_A| \pm 1$. (Since D is checkerboard colorable, there are no single cycle smoothings.) If $|S| = |S_A| - 1$, then $r(S) \leqslant r(S_A) = 0$. Hence $r(S) = 0$ and $k(S) = |S| = |S_A| - 1 = k(S_A) - 1$ as required. Otherwise, if $|S| = |S_A| + 1$, then we claim that $r(S) = 1$ and $k(S) = |S| - 1 = |S_A| = k(S_A)$.

To prove this claim, consider a self-abutting cycle of S_A. This happens only for crossings of D where a white region meets itself. Such a crossing gives rise to a loop γ in the associated Tait graph Γ. We view Γ as a graph embedded in Σ. Since D is reduced, it contains no nugatory crossings, hence the loop γ must be a non-separating curve on Σ. This implies the loop is homologically nontrivial in Σ, namely $[\gamma] \neq 0$ as an element in $H_1(\Sigma)$. Since each cycle in S_A is homologically trivial, the two new cycles formed by switching the smoothing must both carry the homology class $[\gamma]$. In particular, this shows that $r(S) = 1$, and it follows that $k(S) = |S| - r(S) = |S_A| = k(S_A)$. This completes the proof that D is A-adequate.

The same argument applied to the mirror image of D shows that the diagram D is B-adequate.   □

THEOREM 2.9. — *Suppose that L is a link in $\Sigma \times I$ admitting a connected reduced alternating diagram D on Σ. Then* $\mathrm{span}(\langle D \rangle_\Sigma) = 4n - 4g + 4$, *where n is the number of crossings of D and g is the genus of Σ.*

Proof. — Since D is a reduced alternating diagram, it is checkerboard colorable. Further, we can choose the coloring so that the cycles of S_A are the boundaries of the white disks and the cycles of S_B are the boundaries of the black disks. Thus $|S_A|$ is the number of white disks and $|S_B|$ is the number of black disks. The diagram D gives a handlebody decomposition of Σ, and using that to compute the Euler characteristic, we find that $\chi(\Sigma) = n - 2n + |S_A| + |S_B|$. It follows that $|S_A| + |S_B| = n + 2 - 2g$.

By Proposition 2.8, D is adequate, and Corollary 2.7 applies to show that

$$\begin{aligned}
\operatorname{span}(\langle D \rangle_\Sigma) &= 2n + 2(k(S_A) + k(S_B)), \\
&= 2n + 2(|S_A| + |S_B|), \\
&= 4n - 4g + 4. \qquad\qquad \square
\end{aligned}$$

2.3. The dual state lemma

The next result is the analogue of the dual state lemma for surface link diagrams. Note that for a given state S, the dual state, denoted $S^\vee$, is given by performing the opposite smoothing at each crossing. For classical links, the dual state lemma was proved by Kauffman and Murasugi [19, 30]. Our proof is based on the one given by Turaev [35, Section 2].

LEMMA 2.10. — *Let D be a connected link diagram on a surface Σ with genus g, and suppose that D has n crossings. For any state S with dual state $S^\vee$, we have:*

- $|S| + |S^\vee| \leqslant n + 2$.
- $k(S) + k(S^\vee) \leqslant n + 2 - 2g$ *provided that D is cellularly embedded.*

Proof. — Assume the diagram D lies in $\Sigma \times \{1/2\}$ and that its double points (or crossings) have been labeled $c_1, \ldots, c_n$.

Given a state S for D, we construct a compact surface M_S with boundary $\partial M_S = S \cup S^\vee$ embedded in $\Sigma \times I$. The surface is a union of disks and bands, and it has one disk for each crossing and one band for each edge of D. Specifically, if there is an edge of D connecting c_i to c_j, then there is a band of M_S connecting the disk at c_i to the one at c_j. Note that we are not excluding loops, which occur if $c_i = c_j$.

The disks of M_S are assumed to lie in $\Sigma \times \{1/2\}$ and to be pairwise disjoint. The bands of M_S retract to the corresponding edge of D, but they sometimes include a half-twist, as explained below. The bands without twists are assumed to lie in $\Sigma \times \{1/2\}$, and the bands with a half-twist are assumed to lie in a small neighborhood of the associated edge of D. (The direction of the half-twist is immaterial.) From this description, it is clear that there is a deformation retract from M_S to the diagram D.

Let β be a band connecting the disk at c_i to the disk at c_j, and we discuss now whether or not β is flat or twisted as in Figure 2.4. It connects one of outgoing arcs of c_i to one of the incoming arcs of c_j. There are four possibilities, according to whether the outgoing arc from c_i is an
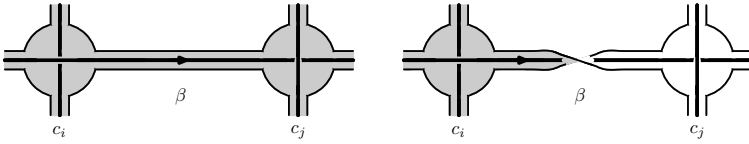
Figure 2.4. The band β connecting the disk at c_i to the disk at c_j. Since the crossings are opposite (over/under), the band will be untwisted if the smoothings are the same (AA or BB) and twisted if the smoothings are opposite (AB or BA).

overcrossing or an undercrossing arc, and whether the incoming arc to c_j is an overcrossing or an undercrossing arc. There are also four possibilities according to the smoothings the state S specifies at c_i and c_j, which is one of $\{AA, AB, BA, BB\}$. The band β will be untwisted if the arcs are opposite (over/under or under/over) and the smoothings are the same (AA or BB), or if arcs are the same (over/over or under/under) and the smoothings are the opposite (AB or BA). Otherwise, the band β includes a half-twist (see Figure 2.4).

This same prescription applies in case β is a loop. In that case, the smoothings at $c_i = c_j$ are necessarily the same, thus the band β will be flat if the outgoing arc at c_i connects to the other incoming arc at $90°$, and it will be half-twisted if it connects to the opposite incoming arc (see Figure 2.5).

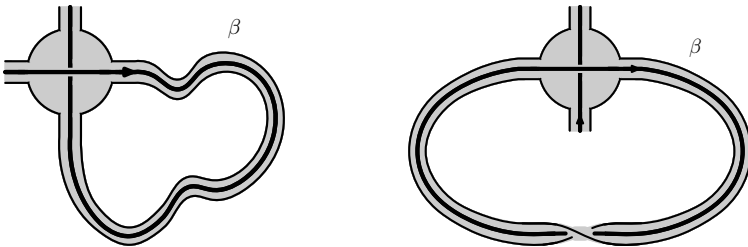Figure 2.5. A flat band and a half-twisted band.

When the surface M_S is defined this way, it follows that $\partial M_S = S \cup S^\vee$. Consider the commutative diagram:

$$(2.7) \quad \begin{array}{ccccc} H_2(M_S, \partial M_S) & \longrightarrow & H_1(\partial M_S) & \longrightarrow & H_1(M_S) & \longrightarrow & \cdots \\ & & \downarrow{\scriptstyle i_*} & & \downarrow{\scriptstyle j_*} & & \\ & & H_1(\Sigma) & \xrightarrow{\;=\;} & H_1(\Sigma) & & \end{array}$$

In the above, all homology groups are taken with $\mathbb{Z}/2$ coefficients, and the top row is the long exact sequence in homology of the pair $(M_S, \partial M_S)$, and the two vertical maps are induced by $M_S \overset{j}{\hookrightarrow} \Sigma \times I \overset{p}{\to} \Sigma$ and $\partial M_S \overset{i}{\hookrightarrow} \Sigma \times I \overset{p}{\to} \Sigma$.

Since M_S is connected and has $\chi(M_S) = n - 2n = -n$, it follows that $b_1(M_S) = b_0(M_S) - \chi(M_S) = n + 1$. Further, $b_2(M_S, \partial M_S) = 1$, thus

$$|S| + |S^\vee| = b_1(\partial M_S) \leqslant b_1(M_S) + b_2(M_S, \partial M_S) = n + 2,$$

which proves part (a).

If D is cellularly embedded, then the map $H_1(D) \to H_1(\Sigma)$ induced by inclusion is surjective. However, since M_S deformation retracts to D, it follows that the map j_* in (2.7) is also surjective. Thus $\dim(\ker j_*) = b_1(M_S) - 2g = n + 1 - 2g$.

By commutativity of (2.7), this implies that

$$k(S) + k(S^\vee) \leqslant \dim(\ker i_*) \leqslant \dim(\ker j_*) + b_2(M_S, \partial M_S) = n + 2 - 2g,$$

which proves part (b). $\qquad\qquad\qquad\qquad\qquad\qquad\qquad\qquad\qquad\qquad\qquad \square$

3. The Jones–Krushkal polynomial

In this section, we recall the Jones–Krushkal polynomial, which is a two-variable Jones-type polynomial associated to oriented links in thickened surfaces and defined in terms of the homological Kauffman bracket [22]. We show that this polynomial, or rather its reduction, has a special form when the link L is checkerboard colorable. We provide many sample calculations, and we prove a result that describes its behavior under horizontal and vertical mirror symmetry.

3.1. The Jones–Krushkal polynomial

DEFINITION 3.1. — *For an oriented link L in a thickened surface $\Sigma \times I$ with link diagram D, the (unreduced) Jones–Krushkal polynomial is given by setting $\widetilde{J}_L(t, z) = \left[(-A)^{-3w(D)} \langle D \rangle_\Sigma \right]_{A = t^{-1/4}}$. Thus, we have*

$$\widetilde{J}_L(t, z) = (-1)^{w(D)} t^{3w(D)/4} \sum_{S \in \mathfrak{S}} t^{(b(S) - a(S))/4} (-t^{-1/2} - t^{1/2})^{k(S)} z^{r(S)}.$$

The usual Jones polynomial is defined similarly:

$$V_L(t) = (-1)^{w(D)} t^{3w(D)/4} \sum_{S \in \mathfrak{S}} t^{(b(S)-a(S))/4} (-t^{-1/2} - t^{1/2})^{|S|-1}.$$

Since $|S| = k(S) + r(S)$, it is clear that one can recover the usual Jones polynomial from $\widetilde{J}_L(t, z)$ by setting $z = -t^{-1/2} - t^{1/2}$ and dividing one $(-t^{-1/2} - t^{1/2})$ factor out.

The factor $t^{3w(D)/4}$ is chosen so that the right hand side of the above equation is invariant under all three Reidemeister moves. Lemma 2.2 implies that the polynomial $\widetilde{J}_L(t, z)$ is invariant under isotopy of links in $\Sigma \times I$. It is also an invariant of diffeomorphism of the pair $(\Sigma \times I, \Sigma \times \{0\})$. By Kuperberg's theorem, we can obtain an invariant of virtual links by calculating the polynomial on a minimal genus representative.

The next lemma shows that the Jones–Krushkal polynomial is a Laurent polynomial in $t^{1/2}$.

LEMMA 3.2. — *If L is an oriented link in $\Sigma \times I$, then it follows that $\widetilde{J}_L(t, z) \in \mathbb{Z}[t^{1/2}, t^{-1/2}, z]$.*

Proof. — Equivalently, we claim that, for any surface link diagram D on Σ, the normalized Kauffman bracket $(-A)^{-3w(D)} \langle D \rangle_\Sigma$ lies in $\mathbb{Z}[A^2, A^{-2}, z]$.

Note that the claim, once proved, implies the lemma. Note further that Equation (2.3) implies that the terms in $\langle D \,|\, S \rangle_\Sigma$ all have the same A-degree modulo 4 for any state $S \in \mathfrak{S}(D)$. For two states $S_1, S_2 \in \mathfrak{S}(D)$, we have $a(S_1) - b(S_1) \equiv a(S_2) - b(S_2) \mod 2$. Hence Equation (2.3) implies that the terms in $\langle D \,|\, S_1 \rangle_\Sigma$ and in $\langle D \,|\, S_2 \rangle_\Sigma$ have the same A-degree modulo 2. Thus, the claim will follow once it has been verified for any one state $S \in \mathfrak{S}(D)$.

We claim that $(-A)^{-3w(D)} \langle D \,|\, S_\sigma \rangle_\Sigma \in \mathbb{Z}[A^2, A^{-2}, z]$, where S_σ is the *Seifert* state. This is the state with all oriented smoothings (see Figure 3.1). (For classical links, S_σ coincides with the one produced by Seifert's algorithm.) As in Figure 3.1, S_σ has A-smoothings at the positive crossings and B-smoothings at the negative crossings. Thus $a(S_\sigma) - b(S_\sigma) = w(D)$.
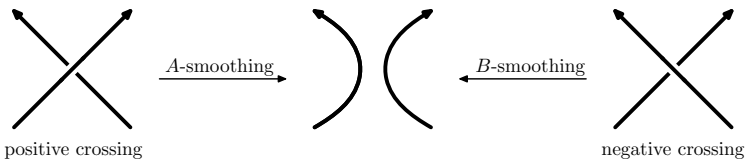

positive crossing   negative crossing

Figure 3.1. Oriented smoothings at positive and negative crossings.

To complete the proof, we apply Equation (2.3) one more time to see that

$$(-A)^{-3w(D)} \langle D \,|\, S_\sigma \rangle_\Sigma = (-A)^{-3w(D)} \left(A^{w(D)} (-A^{-2} - A^2)^{k(S_\sigma)} z^{r(S_\sigma)} \right),$$
$$= (-1)^{w(D)} A^{-2w(D)} (-A^{-2} - A^2)^{k(S_\sigma)} z^{r(S_\sigma)},$$

where the last expression clearly gives an element in $\mathbb{Z}[A^2, A^{-2}, z]$. $\qquad\square$

For a link $L \subset \Sigma \times I$, where Σ has genus g, it follows that $0 \leqslant r(S) \leqslant g$ for all states $S \in \mathfrak{S}$. Thus, we can write $\widetilde{J}_L(t, z) = \sum_{i=0}^{g} \widetilde{\Phi}_i(t) z^i$, where $\widetilde{\Phi}_i(t) \in \mathbb{Z}[t^{-1/2}, t^{1/2}]$ for $i = 0, \ldots, g$ by Lemma 3.2.

PROPOSITION 3.3. — *If L is a link in $\Sigma \times I$ which is not checkerboard colorable, then $\widetilde{\Phi}_0(t) = 0$. Thus $\widetilde{J}_L(t, z) = zJ'(t, z)$, where $J'(t, z) = \sum_{i=1}^{g} \widetilde{\Phi}_i(t) z^{i-1}$.*

If, in addition, L is a link in a thickened torus, then $\widetilde{J}(t, z) = zV_L(t)$ and so is completely determined by the usual Jones polynomial.

Proof. — If L is not checkerboard colorable, then $[L]$ is nontrivial as an element in $H_1(\Sigma)$. The same is true for any state S, since S is homologous to L. Thus $r(S) \geqslant 1$ for all states, which implies that $\Phi_0(t) = 0$. If L is a link in the thickened torus, then it follows that $r(S) = 1$ for all states, thus $\widetilde{J}(t, z) = zV_L(t)$ as claimed. $\qquad\square$

Example 3.4. — Let K be the virtual trefoil (see Figures 1.2 and 2.2). In Example 2.4, we showed that its diagram has homological Kauffman bracket $\langle D \rangle_T = A^2(-A^2 - A^{-2})z + 2z + A^{-2}z$. Since this diagram has writhe $w(D) = -2$, it follows that

$$(3.1) \qquad \widetilde{J}_K(t, z) = z \left(-t^{-5/2} + t^{-3/2} + t^{-1} \right).$$

Since K is not checkerboard colorable and has virtual genus one, Equation (3.1) can also be deduced from Proposition 3.3 and the fact that $V_K(t) = -t^{-5/2} + t^{-3/2} + t^{-1}$.
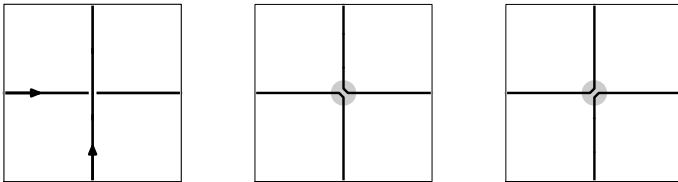

Figure 3.2. A minimal genus diagram of the virtual Hopf link in the torus, and the states S_A and S_B.

Example 3.5. — The virtual Hopf link L (see Figure 1.2) admits a minimal genus diagram D on the torus T which has one crossing. The diagram D, along with the states S_A and S_B, are depicted in Figure 3.2. It has $|S_A| = 1 = |S_B|$ and $r(S_A) = 1 = r(S_B)$, hence $\langle D \rangle_T = Az + A^{-1}z$. Thus, the Jones–Krushkal polynomial of the virtual Hopf link is $\widetilde{J}_L(t,z) = z\left(-t^{-1} - t^{-1/2}\right)$. Since the virtual Hopf link is not checkerboard colorable and has virtual genus one, this also follows from Proposition 3.3 and the fact that $V_L(t) = -t^{-1} - t^{-1/2}$.

3.2. The reduced Jones–Krushkal polynomial

In this section, we introduce a reduction of Jones–Krushkal polynomial for checkerboard colorable links in thickened surfaces.

Suppose that L is a link in $\Sigma \times I$ represented by a checkerboard colorable link diagram D on Σ. Since L is homologically trivial as an element in $H_1(\Sigma \times I; \mathbb{Z}/2)$, it follows that $k(S) \geqslant 1$ for each state S.

DEFINITION 3.6. — *Let L be an oriented, checkerboard colorable link in $\Sigma \times I$ and D a diagram on Σ representing L. The reduced Jones–Krushkal polynomial is defined by setting*

$$J_L(t,z) = (-1)^{w(D)} t^{3w(D)/4} \sum_{S \in \mathfrak{S}} t^{(b(S)-a(S))/4} (-t^{-1/2} - t^{1/2})^{k(S)-1} z^{r(S)}.$$

As before, we can write $J_L(t,z) = \sum_{i=0}^{g} \Phi_i(t)z^i$.

Remark 3.7. — The reduced Jones–Krushkal polynomial $J_L(t,z)$ specializes to the usual Jones polynomial $V_L(t)$ under setting $z = -t^{-1/2} - t^{1/2}$.

In particular, if L is a classical link, then any classical link diagram for L will have $r(S) = 0$ for all states. Thus $J_L(t,z) = V_L(t)$ when L is classical.

For classical links, Jones proved that $V_L(t) \in t^{(m-1)/2}\mathbb{Z}[t,t^{-1}]$, where m is the number of components in L [13, Theorem 2]. This result was extended to checkerboard colorable virtual links by Kamada, Nakabo, and Satoh [17, Proposition 8]. The next result gives the analogous statement for the reduced Jones–Krushkal polynomial.

PROPOSITION 3.8. — *Let L be a checkerboard colorable link with m components in $\Sigma \times I$, and let $J_L(t,z) = \sum_{i=0}^{g} \Phi_i(t)z^i$. Then it follows that $\Phi_i(t) \in t^{(m+i+1)/2}\,\mathbb{Z}[t,t^{-1}]$.*

Proof. — Let D be a checkerboard colorable diagram for L. Lemma 3.2 implies that $\Phi_i(t) \in \mathbb{Z}[t^{1/2}, t^{-1/2}]$. For any state $S \in \mathfrak{S}(D)$, define $\varphi_S(t) \in \mathbb{Z}[t^{1/2}, t^{-1/2}]$ by setting

$$(3.2) \qquad \varphi_S(t) = (-1)^{-3w(D)} t^{3w(D)/4} t^{(b(S)-a(S))/4} (-t^{-1/2} - t^{1/2})^{k(S)-1}.$$

If $S' \in \mathfrak{S}(D)$ is any other state, then we claim that

$$(3.3) \qquad b(S) - a(S) + 2|S| \equiv b(S') - a(S') + 2|S'| \pmod 4.$$

Since any state can be obtained from any other by switching the smoothings at finitely many crossings, it is sufficient to prove (3.3) when S' is obtained from S by switching just one smoothing. In that case, we have $a(S) - b(S) = a(S') - b(S') \pm 2$ and $|S| = |S'| \pm 1$ by checkerboard colorability, and (3.3) follows.

From (3.2), it is clear that $\varphi_S(t) \in t^{(3w(D)+b(S)-a(S)+2k(S)-2)/4} \mathbb{Z}[t, t^{-1}]$.

Let S_σ be the Seifert state with all oriented smoothings (see Figure 3.1). Recall that $b(S_\sigma) - a(S_\sigma) = -w(D)$.

We claim that

$$(3.4) \qquad\qquad\qquad m \equiv |S_\sigma| + n \pmod 2.$$

Each time we perform an oriented smoothing, the number of components changes by one. Thus the claim now follows easily by induction on n.

For any state S, Equation (3.3) implies that

$$(3.5) \qquad b(S) - a(S) + 2|S| = b(S_\sigma) - a(S_\sigma) + 2|S_\sigma| + 4\ell$$

for $\ell \in \mathbb{Z}$. By Equation (3.5) and the fact that $|S| = k(S) + r(S)$, we get that

$$
\begin{aligned}
(3w(D) &+ b(S) - a(S) + 2k(S) - 2)/2 \\
&= (3w(D) + b(S) - a(S) + 2|S| - 2r(S) - 2)/2, \\
&= (2w(D) + 2|S_\sigma| + 4\ell - 2r(S) - 2)/2, \\
&= w(D) + |S_\sigma| + 2\ell - r(S) - 1, \\
&\equiv w(D) + m - n - r(S) - 1 \pmod 2, \\
&\equiv m + r(S) + 1 \pmod 2.
\end{aligned}
$$

(The last two steps use Equation (3.4) and the fact that $n \equiv w(D) \pmod 2$.) We have shown that $\varphi_S(t) \in t^{(m+i+1)/2}\mathbb{Z}[t, t^{-1}]$ for each state S with $r(S) = i$. Since we can write $\Phi_i(t) = \sum_{r(S)=i} \varphi_S(t) z^i$, the proposition now follows. $\qquad\square$
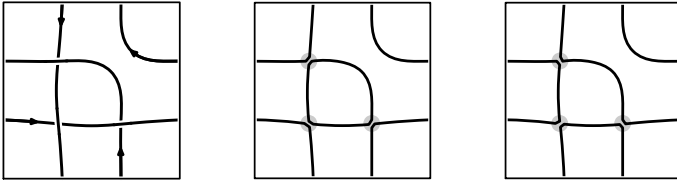
Figure 3.3. A minimal genus diagram of the virtual Borromean rings in the torus, and the states S_A and S_B.

Example 3.9. — The virtual Borromean rings L (see Figure 1.2) admits a minimal genus diagram on the torus T, which is shown in Figure 3.3 along with S_A and S_B. Notice that the diagram is checkerboard colorable, and it has $|S_A| = 2, r(S_A) = 0$, and $|S_B| = 1, r(S_B) = 0$. By direct computation, the three states AAB, ABA, BAA all have $|S| = 1$ and $r(S) = 0$, and the three states ABB, BAB, BBA all have $|S| = 2$ and $r(S) = 1$. Therefore, $\langle D \rangle_T = A^3 d^2 + 3Ad + 3A^{-1}dz + A^{-3}d$, where $d = -A^2 - A^{-2}$. Since D has writhe $w = 3$, it follows that

$$J_L(t, z) = t - 2t^2 - t^3 - 3t^{5/2}z.$$

3.3. Calculations

In this section, we provide some sample calculations of the homological Kauffman bracket and Jones–Krushkal polynomials.
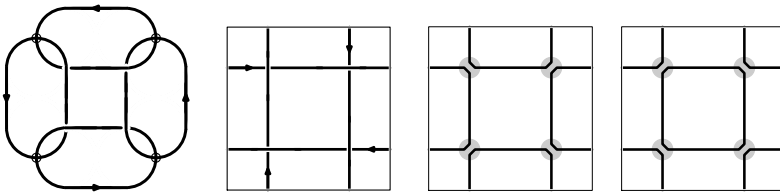

Figure 3.4. From left to right, a virtual link with four components, a minimal genus representative in the torus, and the states S_A and S_B.

Example 3.10. — A virtual link L with four components along with a minimal genus diagram on the torus T appear on the left of Figure 3.4. The states S_A and S_B are shown to the right with shading around the smoothed crossings. From this, we see that $|S_A| = 2 = |S_B|$ and $r(S_A) = 0 = r(S_B)$. Resmoothing one of crossings of S_A, one can show that the four

states $AAAB, AABA, ABAA$, and $BAAA$ all have $|S| = 1$ and $r(S) = 0$. Likewise, resmoothing one of crossings of S_B, one can similarly show that the four states $ABBB, BABB, BBAB$, and $BBBA$ all have $|S| = 1$ and $r(S) = 0$. Resmoothing two of the crossings of S_A (or doing the same to S_B), one can show that the six states $AABB, ABBA, BBAA, BAAB, ABAB, BABA$ all have $|S| = 2$ and $r(S) = 1$. Thus,

$$\langle L \rangle_T = A^4 d^2 + 4A^2 d + 6dz + 4A^{-2}d + A^{-4}d^2,$$

where $d = -A^2 - A^{-2}$.

Since this link has writhe $w(L) = -4$, it follows that

$$J_L(t, z) = t^{-3} \left(t^{-1}(-t^{-1/2} - t^{1/2}) + 4t^{-1/2} + 6z + 4t^{1/2} + t(-t^{-1/2} - t^{1/2}) \right),$$

$$= \left(-t^{-9/2} + 3t^{-7/2} + 3t^{-5/2} - t^{-3/2} \right) + 6t^{-3}z.$$

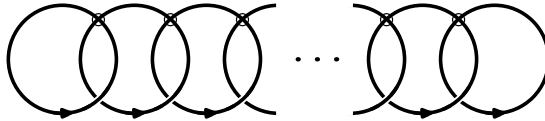The diagram is alternating, therefore it is adequate.

Figure 3.5. The virtual chain link.

Example 3.11. — Figure 3.5 shows a virtual chain link with $m - 1$ crossings and m components. It is not checkerboard colorable, thus it follows that $r(S) \geqslant 1$ for all states. One can further show that its virtual genus is $\lfloor \frac{m}{2} \rfloor$.

Figure 3.6 shows the states S_A and S_B for the virtual chain link. Notice that $|S_A| = 1 = |S_B|$. One can further show that every state S has $|S| = 1$. Since L is not checkerboard colorable, it follows that every state has $r(S) = 1$. As a result we have

$$\langle D \rangle_\Sigma = A^{m-1}z + \binom{m-1}{1}A^{m-3}z + \cdots + \binom{m-1}{m-2}A^{3-m}z + A^{m-1}z,$$

$$= (A + A^{-1})^{m-1}z.$$

Since this link has writhe $w = 1 - m$, we conclude that

$$J_D(t, z) = (-1)^{1-m}t^{(3-3m)/4} \left(t^{-1/4} + t^{1/4} \right)^{m-1} z,$$

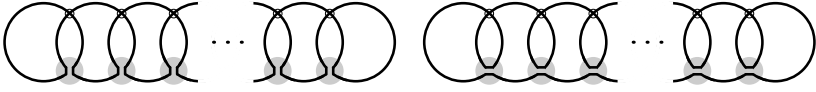$$= (-1)^{m-1} \left(t^{-1} + t^{-1/2} \right)^{m-1} z.$$

Figure 3.6. The states S_A and S_B for the virtual chain link.

3.4. Horizontal and vertical mirror images

In this section, we describe how the Jones–Krushkal polynomial changes under taking mirror images. Recall that there are two ways to take the mirror image of a virtual link L. They are called the vertical and horizontal mirror images, and they are defined in terms of virtual link diagrams as follows.

Given a virtual link diagram D, the vertical mirror image is denoted D^* and it is the diagram obtained by switching the over and under crossing arcs at each classical crossing, see Figure 3.7. The horizontal mirror image is denoted $D^\dagger$ and it is the diagram obtained by reflecting the diagram D across a vertical line $x = x_0$ in $\mathbb{R}^2$ that does not intersect the real or virtual crossings of D, see Figure 3.7.

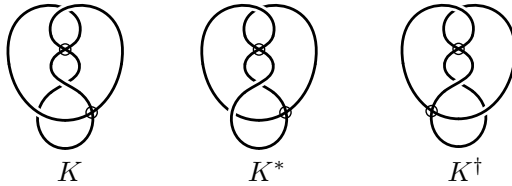

$$K \qquad\qquad K^* \qquad\qquad K^\dagger$$

Figure 3.7. The virtual knot $K = 3.1$ and its mirror images.

We describe these operations for links in thickened surfaces. Let L be a link in $\Sigma \times I$, and let D be its diagram on Σ. Let $\phi\colon \Sigma \times I \to \Sigma \times I$ be the orientation-reversing map given by $\phi(x, t) = (x, 1 - t)$ for $(x, t) \in \Sigma \times I$. Then $\phi(L) = L^*$, the vertical mirror image of L. Now let $\psi\colon \Sigma \to \Sigma$ be an orientation-reversing homeomorphism. (For example, ψ could be reflection through a plane when Σ is embedded in $\mathbb{R}^3$.) Then under $\psi \times \mathrm{id}\colon \Sigma \times I \to \Sigma \times I$, we have $(\psi \times \mathrm{id})(L) = L^\dagger$, the horizontal mirror image of L.

PROPOSITION 3.12. — *If L is a link in $\Sigma \times I$, then*

$$\widetilde{J}_{L^*}(t, z) = \widetilde{J}_L(t^{-1}, z), \quad \text{and} \quad \widetilde{J}_{L^\dagger}(t, z) = \widetilde{J}_L(t^{-1}, z).$$

If L is a checkerboard colored link in $\Sigma \times I$, then

$$J_{L^*}(t, z) = J_L(t^{-1}, z), \quad \text{and} \quad J_{L^\dagger}(t, z) = J_L(t^{-1}, z).$$

Proof. — We give the proof for the vertical mirror image; the proof for horizontal mirror image is similar and left to the reader. Let D be a diagram on Σ for L. Then D^* is obtained by switching the over and under arcs at each crossing of D. Notice that an A-smoothing applied to a crossing of D has the same effect as a B-smoothing applied to the crossing of D^*. Thus, there is a one-to-one correspondence $S \leftrightarrow S^*$ between the state spaces $\mathfrak{S}(D)$ and $\mathfrak{S}(D^*)$, where $S \in \mathfrak{S}(D)$ and $S^* \in \mathfrak{S}(D^*)$ have opposite smoothings at the corresponding crossings of D and D^*.

Clearly, $w(D^*) = -w(D)$, $a(S^*) = b(S)$, and $b(S^*) = a(S)$. Further, we have $|S^*| = |S|$, $k(S^*) = k(S)$, and $r(S^*) = r(S)$. Set $d = -t^{-1/2} - t^{1/2}$. Thus

$$\widetilde{J}_{L^*}(t,z) = (-1)^{w(D^*)} t^{3w(D^*)/4} \sum_{S^* \in \mathfrak{S}(D^*)} t^{(b(S^*)-a(S^*))/4} d^{k(S^*)} z^{r(S^*)},$$

$$= (-1)^{w(D)} t^{-3w(D)/4} \sum_{S \in \mathfrak{S}(D)} t^{(a(S)-b(S))/4} d^{k(S)} z^{r(S)}$$

$$= \widetilde{J}_L(t^{-1}, z).$$

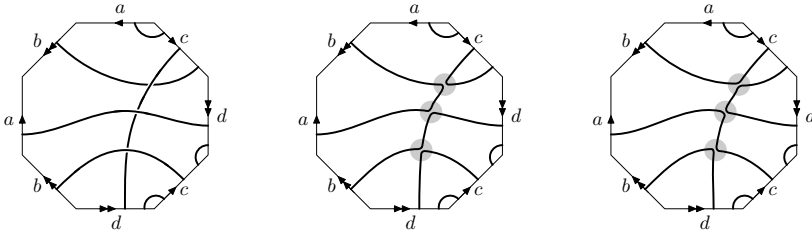The proof for reduced Jones–Krushkal polynomial is similar and is left to the reader. □

Figure 3.8. A minimal genus diagram of 3.1 and the states S_A and S_B.

Example 3.13. — Figure 3.7 shows the virtual knot $K = 3.1$ and its mirror images $K^*, K^\dagger$, and Figure 3.8 shows a minimal genus diagram of K on a genus 2 surface Σ_2. The states S_A and S_B are shown in Figure 3.8 with shading around the smoothed crossings. From that, one can see that $|S_A| = 1, r(S_A) = 1$ and $|S_B| = 1, r(S_B) = 1$. Resmoothing one of the crossings in S_A, one can show that two of the three states AAB, ABA, BAA have $|S| = 1$ and $r(S) = 1$, and the third has $|S| = 2$ and $r(S) = 2$. Resmoothing one of the crossings in S_B, one can further show that two of the three states ABB, BAB, BBA have $|S| = 2$ and $r(S) = 2$, and the third has $|S| = 1$ and $r(S) = 1$.

Since $w(D) = -1$, we have

$$\langle D \rangle_{\Sigma_2} = A^3 z + 2Az + Az^2 + 2A^{-1}z^2 + A^{-1}z + A^{-3}z,$$

$$\widetilde{J}_K(t, z) = -\left(t^{-3/2} + 2t^{-1} + t^{-1/2} + 1\right) z - \left(t^{-1} + 2t^{-1/2}\right) z^2.$$

Thus, Proposition 3.12 applies to show

$$\widetilde{J}_{K^*}(t, z) = \widetilde{J}_{K^\dagger}(t, z) = -\left(1 + t^{1/2} + 2t + t^{3/2}\right) z - \left(2t^{1/2} + t\right) z^2.$$

4. A Kauffman–Murasugi–Thistlethwaite theorem

In this section, we prove the Kauffman–Murasugi–Thistlethwaite theorem for alternating links in surfaces. Throughout this section, Σ denotes a connected closed oriented surface of genus g.

THEOREM 4.1. — *Let L be an oriented link in $\Sigma \times I$, and suppose that D is a connected diagram for L with n crossings. Then*

$$\mathrm{span}(\langle D \rangle_\Sigma) \leqslant 4n + 4 - 4g,$$

with equality if D is reduced and alternating.

Proof. — Let D be a connected diagram for L with n crossings. Then Lemma 2.10 and Corollary 2.7 combine to show that

$$\mathrm{span}(\langle D \rangle_\Sigma) \leqslant 2n + 2k(S_A) + 2k(S_B) \leqslant 4n + 4 - 4g.$$

In case D is also reduced and alternating, then Theorem 2.9 applies to show that

$$\mathrm{span}(\langle D \rangle_\Sigma) = 4n - 4g + 4. \qquad \square$$

COROLLARY 4.2. — *If a link L in $\Sigma \times I$ admits a connected, reduced, alternating diagram with n crossings, then any other diagram for L has at least n crossings.*

Proof. — Let D be a reduced alternating diagram for L with n crossings, then Theorem 4.1 implies that $\mathrm{span}(\langle D \rangle_\Sigma) = 4n - 4g + 4$. If L were to admit a diagram D' with fewer than n crossings, then Theorem 4.1 would apply to show that $\mathrm{span}(\langle D' \rangle_\Sigma) < 4n - 4g + 4$. But $\mathrm{span}(\langle D \rangle_\Sigma) = \mathrm{span}(\langle D' \rangle_\Sigma)$ is independent of the choice of diagram for L, which gives the desired contradiction. $\qquad \square$

We now explain how to deduce that the writhes of two reduced alternating diagrams for the same link in $\Sigma \times I$ are equal.

DEFINITION 4.3. — *Given a link diagram D in $\Sigma \times I$, we define its p-parallel D^p to be the link diagram in $\Sigma \times I$ in which each link component of D is replaced by p parallel copies, with each one repeating the same "over" and "under" behavior of the original component.*

LEMMA 4.4. — *If D is A-adequate, then D^p is also A-adequate. If D is B-adequate, then D^p is also B-adequate.*

Proof. — Let $S_A(D)$ be the pure A-smoothing of D and $S_A(D^p)$ the pure A-smoothing of the p-parallel D^p. It is straightforward to check that $S_A(D^p)$ is the p-parallel of $S_A(D)$. Therefore, if a cycle in $S_A(D^p)$ is self-abutting, then it must be the innermost strand parallel to a self-abutting cycle of $S_A(D)$.

Let S' be the state obtained from $S_A(D)$ by switching the smoothing from A to B, and let S'' be the state obtained from $S_A(D^p)$ by switching the corresponding crossing on the innermost strand. Switching the smoothing at a self-abutting cycle of $S_A(D)$ is either a single-cycle smoothing or increases the number of cycles.

Suppose firstly that it is a single cycle smoothing. (This corresponds to case (c) from the proof of Lemma 2.6.) Notice that the corresponding cycle in $S_A(D^p)$ is not self-abutting. In particular, even though $|S'| = |S_A(D)|$, $k(S') = k(S_A(D))$ and $r(S') = r(S_A(D))$, for the p-strand cable, we have $|S''| = |S_A(D^p)| - 1$. It follows that $k(S'') \leqslant k(S_A(D^p))$ as required.

Now suppose that $|S'| = |S_A(D)| + 1$. (This corresponds to case (b) from the proof of Lemma 2.6.) Since D is A-adequate, the homological rank increases under making the switch from $S_A(D)$ to S'. But S'' has the same homological rank as S', thus the same is true under making the switch from $S_A(D^p)$ to S''. In particular, this shows that $k(S'') \leqslant S_A(D^p)$.

A similar argument can be used to show the second part, namely that if D is B-adequate, then D^p is also B-adequate. The details are left to the reader. □

The next result follows by adapting Stong's argument [32] (cf. [24, Theorem 5.13]). The proof is by now standard, but it is included for the reader's convenience.

THEOREM 4.5. — *Let D and E be two link diagrams on Σ that represent isotopic oriented links in $\Sigma \times I$. If D is A-adequate, then $n_D - w(D) \leqslant n_E - w(E)$, where n_D and n_E are the number of crossings of the diagrams D and E, respectively.*

Proof. — Let $\{L_i \mid i = 1, \dots, m\}$ be the components of L, and let D_i and E_i be the subdiagrams of D and E corresponding to L_i. For each

$i = 1, \ldots, m$, choose non-negative integers μ_i and ν_i such that $w(D_i) + \mu_i = w(E_i) + \nu_i$. Let D'_i be the result of changing D_i by adding μ_i positive kinks, and let E'_i be the result of adding ν_i positive kinks to E_i. Notice that D' is still A-adequate.

The writhes of the individual components satisfy:

$$w(D'_i) = w(D_i) + \mu_i = w(E_i) + \nu_i = w(E'_i),$$

and the contributions from the mixed crossings of D' and E' are both equal to the total linking number $\mathrm{link}(L) = \sum_{i \neq j} \ell k(L_i, L_j)$, which is an invariant of the oriented link L. It follows that $w(D') = w(E')$.

For any $p > 0$, take $(D')^p$ and $(E')^p$. Then $w((D')^p) = p^2 w(D')$, because in forming the p-parallel of a diagram, each crossing is replaced by p^2 crossings of the same sign. The diagrams $(D')^p$ and $(E')^p$, are equivalent and have the same writhe, thus their homological Kauffman brackets must be equal. In particular we have $d_{\max}(\langle (D')^p \rangle_\Sigma) = d_{\max}(\langle (E')^p \rangle_\Sigma)$.

Clearly we have $|S_A(D^p)| = p|S_A(D)| = p\left[k(S_A(D)) + r(S_A(D))\right]$ and $|S_A(E^p)| = p|S_A(E)| = p\left[k(S_A(E)) + r(S_A(E))\right]$. Since

$$r(S_A(D^p)) = r(S_A(D)) \quad \text{and} \quad r(S_A(E^p)) = r(S_A(E)),$$

it follows that

$$k(S_A(D^p)) = |S_A(D^p)| - r(S_A(D^p)) = p(k(S_A(D))) + (p-1)r(S_A(D)),$$
$$k(S_A(E^p)) = |S_A(E^p)| - r(S_A(E^p)) = p(k(S_A(E))) + (p-1)r(S_A(E)).$$

Lemma 2.6 now implies that

$$d_{\max}(\langle (D')^p \rangle_\Sigma) = \left(n_D + \sum_{i=1}^{m} \mu_i \right) p^2 + 2\left(k(S_A(D)) + \sum_{i=1}^{m} \mu_i \right) p - 2r(S_A(D)),$$

$$d_{\max}(\langle (E')^p \rangle_\Sigma) \leqslant \left(n_E + \sum_{i=1}^{m} \nu_i \right) p^2 + 2\left(k(S_A(E)) + \sum_{i=1}^{m} \nu_i \right) p - 2r(S_A(E)).$$

Since this is true for all $p > 0$, comparing coefficients of the p^2 terms, we find that:

$$\text{(4.1)} \qquad n_D + \sum_{i=1}^{m} \mu_i \leqslant n_E + \sum_{i=1}^{m} \nu_i.$$

Subtracting $\sum_{i=1}^{m}(\mu_i + w(D_i)) = \sum_{i=1}^{m}(\nu_i + w(E_i))$ from both sides of (4.1), we get that

$$\text{(4.2)} \qquad n_D - \sum_{i=1}^{m} w(D_i) \leqslant n_E - \sum_{i=1}^{m} w(E_i).$$

Subtracting the total linking number $\text{link}(L)$ from both sides of (4.2) gives the desired inequality. $\qquad\square$

COROLLARY 4.6. — *Let D and E be link diagrams on Σ with n_D and n_E crossings, respectively, for the same oriented link L in $\Sigma \times I$.*

    (i) *If D is A-adequate, then the number of negative crossings of D is less than or equal to the number of negative crossings of E.*

   (ii) *If D is B-adequate, then the number of positive crossings of D is less than or equal to the number of positive crossings of E.*

  (iii) *An adequate diagram has the minimal number of crossings.*

  (iv) *Two adequate diagrams of an oriented link in $\Sigma \times I$ have the same writhe.*

Proof.

(i). — Let, n_+ and n_- be the number of positive and negative crossings, respectively. We have

$$n_D - w(D) \leqslant n_E - w(E),$$
$$n_+(D) + n_-(D) - (n_+(D) - n_-(D)) \leqslant n_+(E) + n_-(E) - (n_+(E) - n_-(E)),$$
$$n_-(D) \leqslant n_-(E).$$

(ii). — Use the negative kinks in the proof of Theorem 4.5. It follows that

$$-n_D + \sum_i \mu_i \geqslant -n_E + \sum_i \nu_i \implies n_D - \sum_i \mu_i \leqslant n_E - \sum_i \nu_i,$$
$$n_D + w(D) \leqslant n_E + w(E) \implies n_+(D) \leqslant n_+(E).$$

(iii). — Follows from (i) and (ii).

(iv). — From (iii), we have $n_D = n_E$. It follows from Theorem 4.5 that

$$n_D - w(D) \leqslant n_E - w(E) \implies w(E) \leqslant w(D).$$

From (ii), we have

$$n_D + w(D) \leqslant n_E + w(E) \implies w(D) \leqslant w(E).$$

Therefore $w(D) = w(E)$. $\qquad\square$

In summary, Corollary 4.2 and Corollary 4.6 establish the first and second Tait Conjectures for reduced alternating links in thickened surfaces.

5. The Tait conjectures for virtual links

In this section, we will prove the first and second Tait conjectures for virtual links using the results from the previous section. Corollary 4.6 gives the desired conclusion for links in a fixed thickened surface, and it remains to extend the statement to stably equivalent links in thickened surfaces.

This will be achieved in two steps. In the first step, we will show that any reduced alternating diagram D of a virtual link L has minimal genus. Thus, Corollary 4.6 applies to show that D has minimal crossing number among all minimal genus diagrams for L. In the second, we will show that any non-minimal genus diagram D' for L has crossing number $n(D') \geqslant n(D)$. This will be proved by relating the spans of $\langle D' \rangle_{\Sigma'}$ and $\langle D \rangle_{\Sigma}$.

For the first step, notice that Corollary 8 of [5] applies and shows that if D is an alternating virtual link diagram for L, then it has minimal genus. Another way is to use a recent result of Adams et al. from [1] to see that any alternating virtual link diagram for L represents a tg-hyperbolic link $\mathscr{L} \subset \Sigma \times I$ in a thickened surface. Therefore, by [2, Theorem 1.2] tg-hyperbolicity implies that this diagram is a minimal genus representative for L.

Either way, we see that any reduced alternating diagram D for L is minimal genus, and Corollary 4.6 implies that any other minimal genus diagram D' for L has $n(D') \geqslant n(D)$.

To complete the proof, we must rule out the possibility of a minimal crossing diagram which is not minimal genus. The following conjecture takes care of that and would lead to a direct proof of the Tait conjectures for virtual links.

CONJECTURE 5.1. — *Given a virtual link L, any minimal crossing diagram for it has minimal genus.*

Conjecture 5.1 is known to be true for virtual knots. The proof is due to Manturov and uses homological parity [28]. As a consequence, we can give a simple proof of Tait's first and second conjectures for virtual knots.

THEOREM 5.2. — *Suppose that K is a virtual knot admitting an adequate diagram D on a minimal genus surface Σ with crossing number $n(D)$ and writhe $w(D)$. Then any other diagram D' for K has crossing number $n(D') \geqslant n(D)$. If D_1 and D_2 are two adequate diagrams of minimal genus for K, then $n(D_1) = n(D_2)$ and $w(D_1) = w(D_2)$.*

Proof. — If D' is a minimal crossing diagram for K, then Conjecture 5.1 implies D' has minimal genus. Therefore, since D is also a minimal genus diagram, Corollary 4.6 (iii) applies to show that $n(D) \leqslant n(D')$. If D_1 and D_2 are two adequate diagrams of minimal genus for K, then Corollary 4.6 applies to show that $n(D_1) = n(D_2)$ and $w(D_1) = w(D_2)$. $\qquad\square$

We will now show how to prove the Tait conjectures for virtual links without assuming Conjecture 5.1. This is achieved by developing an alternative approach that involves comparing the spans of the homological brackets of links related by stabilization moves.

To that end, observe firstly that the homological Kauffman bracket is an invariant of unoriented links in thickened surfaces under regular isotopy, and that the Jones–Krushkal polynomial $\widetilde{J}_L(t, z)$ is an invariant of oriented links under isotopy and diffeomorphism of the thickened surface. As we have seen, however, neither is invariant under stabilization or destabilization.

Suppose then that L is a virtual link and D is representative link diagram on a surface Σ. By the Kamada–Kamada construction, we can assume that the inclusion map $D \hookrightarrow \Sigma$ is a cellular embedding (cf. Remark 1.6).

If D is not a minimal genus diagram for L, then it must admit a destabilizing curve γ. Let D' be the link diagram on the destabilized surface Σ' of genus $g - 1$ obtained by destabilizing Σ along γ. Then it follows that the homological Kauffman brackets and Jones–Krushkal polynomials of D and D' are related to one another in a more-or-less straightforward way. Namely, the bracket $\langle D' \rangle_{\Sigma'}$ is obtained from $\langle D \rangle_\Sigma$ by replacing z by $-A^2 - A^{-2}$ in some of the terms. The Jones–Krushkal polynomials are related in a similar fashion. Specifically, let U be the subspace of $H_1(\Sigma)$ generated by $[\gamma]$ and its Poincaré dual and suppose that $S \in \mathfrak{S}(D)$ is a state for D such that $i_*(H_1(S)) \cap U \neq 0$. Then under destabilization, if the homological rank of S drops by one, then we substitute one z-factor in $\langle D \rangle_\Sigma$ with $-A^2 - A^{-2}$. Otherwise, if $i_*(H_1(S)) \cap U = 0$, then the homological rank does not change and we do not make the substitution. In either case, we see that $\mathrm{span}(\langle D' \rangle_{\Sigma'}) \leqslant \mathrm{span}(\langle D \rangle_\Sigma) + 4$.

Repeat this argument until a minimal genus diagram is obtained. (This step uses Kuperberg's proof of Theorem 1.2, which tells us that any non-minimal genus representative can be repeatedly destabilized to obtain a minimal genus representative.) Therefore, suppose that $\gamma_1 \ldots, \gamma_\ell$ are destabilizing curves for D, and let D' be the link diagram on the surface Σ' obtained by destabilizing Σ along $\gamma_1 \ldots, \gamma_\ell$. Notice that Σ' has genus $g' = g - \ell$ and it is by assumption a surface of minimal genus for L.

Then as explained above, the bracket $\langle D' \rangle_{\Sigma'}$ can be obtained from $\langle D \rangle_\Sigma$ by substituting $z = -A^2 - A^{-2}$ for up to ℓ of the z-factors in the terms $\langle D \,|\, S \rangle_\Sigma$ for any given state $S \in \mathfrak{S}(D)$. The number of z-factors requiring substitution in $\langle D \,|\, S \rangle_\Sigma$ is equal to the dimension of $i_*(H_1(S)) \cap U$, where $U \subset H_1(\Sigma)$ is the symplectic subspace generated by $[\gamma_1], \ldots, [\gamma_\ell]$. (Note that $\dim U = 2\ell$, since it also contains the Poincaré duals of $[\gamma_1], \ldots, [\gamma_\ell]$.) With each substitution the span of $\langle D \,|\, S \rangle_\Sigma$ increases by four, thus it follows that $\mathrm{span}(\langle D' \rangle_{\Sigma'}) \leqslant \mathrm{span}(\langle D \rangle_\Sigma) + 4\ell$.

Lemma 2.10 and Corollary 2.7 imply that

$$\mathrm{span}(\langle D \rangle_\Sigma) \leqslant 4(n - g) + 4, \tag{5.1}$$

where $n = n(D)$ is the crossing number of D and $g = g(\Sigma)$ is the genus of Σ.

Now suppose that D'' is an adequate diagram for L on a minimal genus surface. Since D' is also a minimal genus diagram for L, Theorem 1.2 implies that D'' and D' represent equivalent links in $\Sigma' \times I$. Therefore

$$\mathrm{span}(\langle D'' \rangle_{\Sigma'}) = \mathrm{span}(\langle D' \rangle_{\Sigma'}) \leqslant \mathrm{span}(\langle D \rangle_\Sigma) + 4\ell. \tag{5.2}$$

In addition, Theorem 2.9 implies that

$$\mathrm{span}(\langle D'' \rangle_{\Sigma'}) = 4(n'' - g') + 4 = 4(n'' - g + \ell) + 4, \tag{5.3}$$

where $n'' = n(D'')$ is the crossing number of D''.

Therefore, by Equations (5.1), (5.2), and (5.3), we see that

$$\begin{aligned} \mathrm{span}\left(\langle D'' \rangle_{\Sigma'}\right) = 4(n'' - g + \ell) + 4 &\leqslant \mathrm{span}(\langle D \rangle_\Sigma) + 4\ell \\ &\leqslant 4(n - g) + 4\ell + 4. \end{aligned} \tag{5.4}$$

Thus, we conclude from this that $n'' \leqslant n$.

THEOREM 5.3. — *Suppose that L is a virtual link admitting an adequate diagram D on a minimal genus surface Σ with crossing number $n(D)$ and writhe $w(D)$. Then any other diagram D' for L has crossing number $n(D') \geqslant n(D)$. If D_1 and D_2 are two adequate diagrams of minimal genus for L, then $n(D_1) = n(D_2)$ and $w(D_1) = w(D_2)$.*

Remark 5.4. — In the classical setting, Thistlethwaite proved the following stronger result, namely that a classical link L is alternating and prime if and only if $\mathrm{span}(V_K(t)) = c(L)$, the crossing number of L. One can see by example that this result is not true for virtual knots. In particular, the virtual knots 4.98 and 4.107 are both checkerboard colorable, prime and have the same crossing number and reduced Jones–Krushkal polynomial (see Table 5.2). However, 4.107 is alternating and 4.98 is not.

A natural question is whether the Tait flyping conjecture can also be extended to alternating virtual links. The flype move is shown in Figure 5.1. For tangles that contain only classical crossings, it is immediate that the flype move does not alter the virtual link type. When the tangle contains virtual crossings, the flype move can change the virtual link type. (This was already noted by Zinn-Justin and Zuber in [36].)

The analogue of the Tait flyping conjecture is therefore the assertion that any two reduced alternating link diagrams of the same link are related by a sequence of flype moves by classical tangles.

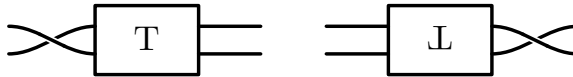QUESTION 5.5. — *Is the Tait flyping conjecture true for alternating virtual links?*

Figure 5.1. *The flype move for virtual links, where "T" is a classical tangle diagram.*

In a different direction, one can ask whether the Tait conjectures continue to hold in the welded category.

QUESTION 5.6. — *Are the Tait conjectures true for alternating welded links?*

Another interesting question is whether the Jones–Krushkal polynomial is a virtual unknot detector. Proposition 3.3 shows that a virtual knot that is not checkerboard colorable has nontrivial Jones–Krushkal polynomial.

QUESTION 5.7. — *Does there exist a checkerboard colorable virtual knot K which is nontrivial and has $J_K(t, z) = 1$?*

For classical knots, this is equivalent to the open problem which asks whether the Jones polynomial is an unknot detector.

For classical links, Khovanov defined a homology theory that categorifies the Jones polynomial. The result is a bigraded homology theory of links that is known to detect the classical unknot [21]. Khovanov homology has been extended to virtual knots and links (see [26, 27]), and it categorifies the usual Jones polynomial for virtual links. However, the resulting knot homology does not detect the virtual unknot.

An interesting problem would be to construct a triply graded homology theory for links in thickened surfaces that categorifies the Jones–Krushkal polynomial. In particular, is the resulting knot homology theory sufficiently strong to detect the virtual unknot?

In closing, Table 5.1 presents the Jones–Krushkal polynomials for virtual knots with up to three crossings and Table 5.2 the reduced Jones–Krushkal polynomial for checkerboard colorable virtual knots with up to four crossings.

Acknowledgements

Table 5.1. *The Jones–Krushkal polynomials for virtual knots with up to three crossings. Note that 3.5, **3.6**, and 3.7 are checkerboard colorable, and their reduced Jones–Krushkal polynomial is listed first. The knot **3.6** in boldface is classical.*

Virtual Knot	$\widetilde{J}_K(t, z)$
2.1	$(-t^{-5/2} + t^{-3/2} + t^{-1})z$
3.1	$-(t^{-3/2} + 2t^{-1} + t^{1/2} + 1)z - (t^{-1} + 2t^{-1/2})z^2$
3.2	$(t^{-2} - t^{-1} + 1 - t + t^2)z$
3.3	$-(t^{-3} + 2t^{-5/2} + 2t^{-2})z - (t^{-5/2} + t^{-2} + t^{-3/2})z^2$
3.4	$-(3t^{-1} + 2t^{-1/2})z - (t^{-3/2} + t^{-1/2} + 1)z^2$
3.5	$\left((t^{-3} - 2t^{-2}) + (t^{-7/2} - t^{-5/2} - t^{-3/2})z\right)\left(-t^{1/2} - t^{-1/2}\right)$
3.6	$\left(-t^{-4} + t^{-3} + t^{-1}\right)\left(-t^{1/2} - t^{-1/2}\right)$
3.7	$\left((t^{-2} - t^{-1} - 1) + (t^{-3/2} - 2t^{-1/2})z\right)\left(-t^{1/2} - t^{-1/2}\right)$

Table 5.2. *The reduced Jones–Krushkal polynomials for checkerboard colorable virtual knots with four crossings. The knot **4.108** in boldface is classical.*

Virtual Knot	$J_K(t, z)$
4.85	$(3t^{-2} + 2t^{-1}) + (t^{-5/2} + 6t^{-3/2} + t^{-1/2})z + (t^{-2} + 2t^{-1})z^2$
4.86	$(-t^{-1} + 2 - 2t) + (-t^{-3/2} + t^{-1/2} - t^{3/2})z$
4.89	$(t^{-4} + 4t^{-3}) + (4t^{-7/2} + 4t^{-5/2})z + (2t^{-3} + t^{-2})z^2$
4.90	$5 + (4t^{-1/2} + 4t^{1/2})z + (t^{-1} + 1 + t)z^2$
4.98	$(t^{-1} + 3 + t) + (4t^{-1/2} + 4t^{1/2})z + 3z^2$
4.99	$(-t^{-1} + 3 - t) + (-t^{-3/2} + t^{-1/2} + t^{1/2} - t^{3/2})z$
4.105	$(t^{-4} + t^{-3} - 2t^{-2} + t^{-1}) + (2t^{-7/2} - 2t^{-5/2})z$
4.106	$(-t^{-3} + t^{-2} - 1) + (-t^{-5/2} + 2t^{-3/2} - 2t^{-1/2})z$
4.107	$(t^{-1} + 3 + t) + (4t^{-1/2} + 4t^{1/2})z + 3z^2$
4.108	$t^{-2} - t^{-1} + 1 - t + t^2$

BIBLIOGRAPHY

[1] C. ADAMS, C. ALBORS-RIERA, B. HADDOCK, Z. LI, D. NISHIDA, B. REINOSO & L. WANG, "Hyperbolicity of links in thickened surfaces", *Topology Appl.* **256** (2019), p. 262-278.

[2] C. ADAMS, O. EISENBERG, J. GREENBERG, K. KAPOOR, Z. LIANG, K. O'CONNOR, N. PACHECO-TALLAJ & Y. WANG, "tg-hyperbolicity of virtual links", *J. Knot Theory Ramifications* **28** (2019), no. 12, article no. 1950080 (26 pages).

[3] C. ADAMS, T. FLEMING, M. LEVIN & A. M. TURNER, "Crossing number of alternating knots in $S \times I$", *Pac. J. Math.* **203** (2002), no. 1, p. 1-22.

[4] H. U. BODEN, R. I. GAUDREAU, E. HARPER, A. J. NICAS & L. WHITE, "Virtual knot groups and almost classical knots", *Fundam. Math.* **138** (2017), p. 101-142.

[5] H. U. BODEN & H. KARIMI, "A characterization of alternating links in thickened surfaces", *Proc. R. Soc. Edinb., Sect. A, Math.* (2021), `https://doi.org/10.1017/prm.2021.78`, first view.

[6] J. S. CARTER, S. KAMADA & M. SAITO, "Stable equivalence of knots on surfaces and virtual knot cobordisms", *J. Knot Theory Ramifications* **11** (2002), no. 3, p. 311-322, Knots 2000 Korea, Vol. 1 (Yongpyong).

[7] S. CHMUTOV & I. PAK, "The Kauffman bracket of virtual links and the Bollobás-Riordan polynomial", *Mosc. Math. J.* **7** (2007), no. 3, p. 409-418.

[8] S. CHMUTOV & J. VOLTZ, "Thistlethwaite's theorem for virtual links", *J. Knot Theory Ramifications* **17** (2008), no. 10, p. 1189-1198.

[9] H. A. DYE, "Checkerboard framings and states of virtual link diagrams", in *Knots, links, spatial graphs, and algebraic invariants*, Contemporary Mathematics, vol. 689, American Mathematical Society, 2017, p. 53-64.

[10] H. A. DYE & L. H. KAUFFMAN, "Minimal surface representations of virtual knots and links", *Algebr. Geom. Topol.* **5** (2005), p. 509-535.

[11] M. GOUSSAROV, M. POLYAK & O. VIRO, "Finite-type invariants of classical and virtual knots", *Topology* **39** (2000), no. 5, p. 1045-1068.

[12] J. GREEN, "A table of virtual knots", 2004, `http://www.math.toronto.edu/drorbn/Students/GreenJ`.

[13] V. F. R. JONES, "A polynomial invariant for knots via von Neumann algebras", *Bull. Am. Math. Soc.* **12** (1985), no. 1, p. 103-111.

[14] N. KAMADA, "On the Jones polynomials of checkerboard colorable virtual links", *Osaka J. Math.* **39** (2002), no. 2, p. 325-333.

[15] ———, "Span of the Jones polynomial of an alternating virtual link", *Algebr. Geom. Topol.* **4** (2004), p. 1083-1101.

[16] N. KAMADA & S. KAMADA, "Abstract link diagrams and virtual knots", *J. Knot Theory Ramifications* **9** (2000), no. 1, p. 93-106.

[17] N. KAMADA, S. NAKABO & S. SATOH, "A virtualized skein relation for Jones polynomials", *Ill. J. Math.* **46** (2002), no. 2, p. 467-475.

[18] H. KARIMI, "The Khovanov homology of alternating virtual links", *Mich. Math. J.* **70** (2021), no. 4, p. 749-778.

[19] L. H. KAUFFMAN, "State models and the Jones polynomial", *Topology* **26** (1987), no. 3, p. 395-407.

[20] ———, "Virtual knot theory", *Eur. J. Comb.* **20** (1999), no. 7, p. 663-690.

[21] P. B. KRONHEIMER & T. S. MROWKA, "Khovanov homology is an unknot-detector", *Publ. Math., Inst. Hautes Étud. Sci.* (2011), no. 113, p. 97-208.

[22] V. KRUSHKAL, "Graphs, links, and duality on surfaces", *Comb. Probab. Comput.* **20** (2011), no. 2, p. 267-287.

[23] G. Kuperberg, "What is a virtual link?", *Algebr. Geom. Topol.* **3** (2003), p. 587-591.

[24] W. B. R. Lickorish, *An introduction to knot theory*, Graduate Texts in Mathematics, vol. 175, Springer, 1997, x+201 pages.

[25] V. O. Manturov, "Kauffman-like polynomial and curves in 2-surfaces", *J. Knot Theory Ramifications* **12** (2003), no. 8, p. 1145-1153.

[26] ———, "The Khovanov polynomial for virtual knots", *Dokl. Akad. Nauk SSSR* **398** (2004), no. 1, p. 15-18.

[27] ———, "Khovanov's homology for virtual knots with arbitrary coefficients", *Izv. Ross. Akad. Nauk, Ser. Mat.* **71** (2007), no. 5, p. 111-148.

[28] ———, "Parity and projection from virtual knots to classical knots", *J. Knot Theory Ramifications* **22** (2013), no. 9, article no. 1350044 (20 pages).

[29] W. Menasco & M. B. Thistlethwaite, "The classification of alternating links", *Ann. Math.* **138** (1993), no. 1, p. 113-171.

[30] K. Murasugi, "Jones polynomials and classical conjectures in knot theory", *Topology* **26** (1987), no. 2, p. 187-194.

[31] W. Rushworth, "Doubled Khovanov homology", *Can. J. Math.* **70** (2018), no. 5, p. 1130-1172.

[32] R. Stong, "The Jones polynomial of parallels and applications to crossing number", *Pac. J. Math.* **164** (1994), no. 2, p. 383-395.

[33] P. G. Tait, *On Knots I, II, III, Scientific papers, Vol I*, Cambridge University Press, 1898, 273-347 pages.

[34] M. B. Thistlethwaite, "A spanning tree expansion of the Jones polynomial", *Topology* **26** (1987), no. 3, p. 297-309.

[35] V. G. Turaev, "A simple proof of the Murasugi and Kauffman theorems on alternating links", *Enseign. Math.* **33** (1987), no. 3-4, p. 203-225.

[36] P. Zinn-Justin & J.-B. Zuber, "Matrix integrals and the generation and counting of virtual tangles and links", *J. Knot Theory Ramifications* **13** (2004), no. 3, p. 325-355.

Hans U. BODEN
Mathematics & Statistics
McMaster University
Hamilton, Ontario (Canada)
boden@mcmaster.ca

Homayun KARIMI
Mathematics & Statistics
McMaster University
Hamilton, Ontario (Canada)
karimih@math.mcmaster.ca